Mechanisms In Creep And Hot Working To High Strain; Microstructural Evidence, Inconsistencies Part II: Contrasts In Hot Worked Microstructures: EOM, POM, XRD, TEM, STEM, SEM-EBSI AND OIM

H. J. McQueen, Concordia University, Montreal, Canada

ABSTRACT

Substructure characteristics in hot worked Al alloys are very important for modeling mechanical properties during hot forming, and also in the product. In contrast to simple grain shape in etched-optical microscopy (EOM), polarized optical microscopy (POM) significantly confirmed subgrain presence in better detail than x-ray diffraction (XRD). Transmission electron microscopy (TEM) revealed the dislocations forming subgrain boundaries (SGB) and dispersed between them; TEM in scanning mode (STEM) could provide microtextures substantiating XRD. Scanning electron microscopy with back-scattered image (SEM-EBSI) exhibited substructures more accurately than POM but much less detailed than TEM. Finally, orientation-imaging microscopy (OIM) provided microstructures as in SEM-EBSI and also detailed misorientations; however, omission of very-low angle SGB seen in TEM gave rise to estimates of larger subgrain sizes and misorientations. The field of view is very limited in TEM, but fairly similar in POM, SEM-EBSI and OIM although higher magnifications are possible in the last two. The various techniques are also affected differently by substructure scale (temperature, strain and rate) and composition that also influence specimen preparation. Examination by several techniques is best assurance of correct interpretation of microstructural characteristics.

RIASSUNTO

Nel corso della lavorazione a caldo delle leghe di alluminio, la conoscenza delle caratteristiche della sottostruttura si rivela molto importante per la modellazione delle proprietà meccaniche sia durante la formatura che nel prodotto finale. In contrasto con la semplice forma del grano, rilevata con microscopia ottica di superfici attaccate chimicamente (EOM), la microscopia ottica polarizzata (POM) evidenzia chiaramente la presenza di sottograni con maggior dettagli rispetto a quelli forniti dalla diffrazione a raggi X (XRD). La microscopia elettronica in trasmissione (TEM) mette in evidenza le dislocazioni sia organizzate in confini che disperse all'interno di sottograni (SGB); il TEM, nella versione scanner (STEM), evidenzia le micro tessiture, confermando XRD. Il microscopio elettronico a scansione, equipaggiato con rivelatori di immagini retrodiffuse (SEM-EBSI), mostra sottostrutture in modo più accurato di POM ma con meno dettagli di TEM. La microscopia ad orientazione di immagini (OIM) è in grado di evidenziare microstrutture e disorientazioni accurate come SEM-EBSI; la mancata rilevazione dei SGB caratterizzati da disorientazione molto piccola, rilevata con il TEM, ha portato in passato a stime maggiori sia delle dimensioni che della disorientazione dei grani. Il campo osservabile, piuttosto limitato nel TEM, è abbastanza simile nel POM, SEM-EBSI e OIM anche se le due ultime consentono di ottenere ingrandimenti maggiori. Le diverse tecniche sono, in modo diverso, influenzate anche dalla dimensione della sottostruttura, (funzione della temperatura, deformazione, velocità di deformazione), e composizione che anche influenza la preparazione dei provini da osservare. Le indagini effettuate con le diverse tecniche sono la miglior garanzia della corretta interpretazione delle caratteristiche microstrutturali.

KEYWORDS

Hot Working, Aluminum Alloys, Dynamic Recovery, Transition Boundaries, Polarized Optical Microscopy, Transmission Electron Microscopy, Scanning Electron Microscopy, Orientation Imaging Microscopy.

INTRODUCTION

Dislocation aggregates are examined as in hot working with some clarification from observations in creep and cold working that have been examined earlier and in greater frequency.

The techniques include X-ray diffraction (XRD), etched optical microscopy (EOM), polarized optical microscopy (POM), transmission electron microscopy (TEM) scanning STEM, scanning electron microscopy - electron back scattering (SEM-EBS) and orientation imaging microscopy (OIM), with which the author has experience. Of these, only TEM images dislocations directly; the others depend on misorientations ψ on opposite sides of dislocation walls. Strain induced boundaries (SIB) consisting of dislocations, serve as barriers, trapping or releasing dislocations; they may build up by accretion and merging to create high-angle boundaries that may develop high mobility in nucleation. The following mechanisms during straining at elevated temperature T

were explained in Part I: dynamic recovery (DRV); dynamic recrystallization (DRX); discontinuous (dDRX); continuous (cDRX); and grain defining (gDRV) (formerly geometric gDRX) as well as those occurring afterwards, static recovery (SRV) and recrystallization (SRX).

For these theories, metallographic problems created confusions for periods of time but new techniques with different capabilities inspired reexamination leading to successful clarification.

The objectives are to look at the unit dislocation mechanisms (cross slip, climb, subgrain boundary (SGB) formation and rearrangement) that are significant in hot working dependent on temperature T and strain rate $\dot{\varepsilon}$ that control flow stress σ and ductility ε_F, thus defining the process practice and the substructure, grain shape/size and texture that cause product properties.

In Part I, these have been itemized in order of progression with strain and with complexity of interaction; they will be referred to by the subsection notation system found there: {DRV}; {DBTB}, deformation bands + transition boundaries (TB); {SERV}, serrations + DRV; {DRX}.

The detailed sub-goals are as follows:

1. to explain the dislocation behaviors discovered by each microscopic technique in a historic context;
2. to point out the deficiencies of the techniques and explain how hypotheses were clarified by new techniques (sometimes inadequate understanding and over-enthusiasm for a novel method created inconsistencies);
3. to bring the results of the various techniques into an integrated theory of dislocation substructure formation explaining elevated T characteristics notably steady-state stress σ_S, thus providing a guide to extended research and improved application.

ETCHED OPTICAL MICROSCOPY (EOM) - X-RAY DIFFRACTION (XRD)

By about 1955, EOM had provided significant information on grain shape change in deformation and on nucleation and growth of new grains in static recrystallization (SRX) during annealing. In cold worked Al and α-Fe, initial softening occurred, more at low T, without any change in grain structure. XRD showed line broadening in cold work, sharpening from SRV in annealing and break up into spots in SRX [1-3]. The questions and incomplete theories of the period (such as Mehl [3], Schmid & Boas [4], Perryman [5], Barrett [2], Sachs & Van Horne [6]) have been thoroughly reviewed for their pertinence to hot working [7-11]. After hot working, the grains in Al alloys and ferritic steels were frequently elongated but were much softer than after similar cold work, yet on annealing they recrystallized, although more slowly and to larger grains [12-16]. Flow curves at high temperature (T_D) exhibited reduced strain hardening and attainment of a steady state (ε, $\dot{\varepsilon}$, T constant) similar to creep [4,17-22].

At mid-century, XRD was able to show that subgrains formed during creep, attaining a constant size in steady state; size was larger at higher T or lower σ [2, 7, 23-27]. Polygonization in recovery annealing of cold worked metal was discovered and shown to be similar to subgrain formation in creep [1, 2, 7, 28-31]. Ultimately it was shown that in steady state, size depended not only on σ but also on Z ($\dot{\varepsilon}$ exp (Q/RT) (Part I: 1, 2-DRV), [25-27] with activation energy Q defined by Dorn and others [32, 33]. In this period, XRD provided structure averaged over a broad region thus unable to provide detailed dislocation arrangements. EOM of hot torsioned Fe-25Cr [21], hot compression of α-Fe and Fe-3Si [11, 34] and creeped Fe-3Si [25, 35] showed development of subgrains, the last two being confirmed by TEM. In Fe-25Cr, the subgrains remained constant in size to high strains, finally masking the serrated GB; this was mistaken for DRX, although XRD denied that interpretation. [21,36]. EOM of 409, 430 and 434 steels showed elongated grains (ε = 4) some with small subgrains and others with large ones as if SRX but TEM confirmed all were DRV [37, 38].

After limited experimental straining, EOM discovered planar and wavy slip lines, formation of kinks and deformation bands [1, 39-41] (Part I: 1, 2-DBTB); however, improper polishing could introduce artifacts [1,40]. Etch pitting (limited to low strains) showed dislocation rearrangement from slip planes to recovered walls [1,39,41]. The spacing of slip bands diminished with strain but their width increased [39,42]. The distance between bands in Al (ε = 15%) rose from 2 μm at 20°C to 10 μm at 500°C, whereas on adding Mg (ε = 35%) it decreased from 3 to 1.6 μm at 5%. In Al single crystals, much more so than in lower SFE metals, cross slip caused bands to deviate and to split; in some cases kinks, inclined to the initial slip lanes, developed growing in length and width (one form of deformation band) [39]. Slip on a primary and a secondary system developed in single crystals with tension axis near the {100}-{111} zone, in some cases forming defined deformation bands (Part I: 2, 3-DBTB); crystals far from that zone slipped on one system even when the lattice rotated to or beyond that circle [39] (until causing microbands to form as discussed later in polycrystals). For deformation bands, the rotations were followed by XRD [43,44] and also their influence on SRX [28,29].

POLARIZED OPTICAL MICROSCOPY - POM

Starting from about 1955, polarized optical microscopy (POM) of anodized specimens of recrystallized Al was able to show different orientations of grains either in shades of grey or in colors with a quarter wave plate [45]. It appeared that the birefringent Al_2O_3 layer nucleated at many points but grew into a unified whole over each grain. No defined relation between the 2-d oxide layer and the 3-d lattice has been confirmed [46]. In hot worked Al, variously shaded subgrains were exhibited in elongated grains, as previously noted in extrusion and rolling. At very low strains in Al (400°C), contrasting bands appeared in some isolated grains, but being only one subgrain thick, did not remain stable or appear for ε > 0.1 [47-50]. The size was larger as T increased or $\dot{\varepsilon}$, Z decreased in consistency with XRD results in creep [7, 11, 17, 20, 49, 50]. Above 350°C, the subgrains were equiaxed in specimens compressed [22], torsioned [17, 48,51-55], rolled [14,15] or extruded [49,50,56] with ε ranging from 0.7 to 10 (Part I: 1-3,7 DRV) (Fig. 1). Replicas of anodized specimens examined in TEM exhibited cubes related to the lattice in SRX grains and in elongated grains extruded above 400°C, but a sinuous roped structure below 300°C

[56]. At lower T, POM exhibits a wood grain structure at about 100X but the subgrains are too vague to be resolvable at higher magnifications [49,57]. In hot rolling that finished at 0.55 or 0.65 T_M to 90% reduction (ε = 2.3) in one pass, Al exhibited elongated grains with subgrains that were stable in annealing at T_D for many hours [14,15]. On the other hand Cu and Ni with low stacking fault energy (SFE) retained elongated grains with strain markings (EOM) only if quenched and highly refined SRX grains within seconds [15]. In torsion to high strains, Cu and Ni exhibited DRX grains on quenching (EOM) and in Al, the POM subgrains caused such GB serrations that they were mistaken for DRX grains (discussed under serrations and SGB) [17]; although this was later rescinded [58] it gave rise to confusion for many years [18]. POM of anodized Ni has shown the presence of deformation bands, of subgrains and of serrated GB when quenched under stress to prevent SRX [47]. Since POM provided shading in some degree related to underlying crystalline orientation and subgrain sizes reasonably related to straining conditions, it was utilized to estimate misorientation Ψ between subgrains. As contrast seemed to rise with strain in steady state, it was interpreted that Ψ increased [59, 60]. This gave rise to the theory that SGB played no role in defining creep strength that still persists [25, 31, 60-62], although in cold working the various dislocation walls are believed to cause strain hardening [62-64]. Studies in depth have shown that the contrast of subgrains is strongly dependent on the angle between the polarizer's, maximizing near extinction at 90° [46]. Results from TEM at the period [14, 15, 22, 49, 50, 55, 60] and more extensive results later (Part I: 6, 7-DRV) have not conclusively resolved the matter (discussed later under serrations on SGB). POM has played, and continues to play, a valuable role in giving a large field of view of strain homogeneity (or lack of it), of grain shape and of subgrains in Al and many alloys at strains up to 4 above 350°C [48, 52, 53]. The problems of POM for Al-5Mg are discussed under SEM-EBSI that along with

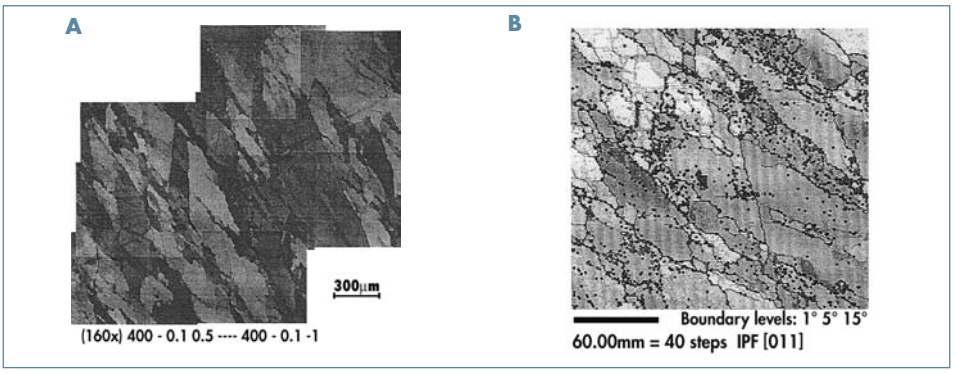

Fig. 1: Specimens of Al deformed at 400°C 0.1s^{-1} deformed to ε = 1 exhibit elongated grains with deformation bands, subgrains and serrated boundaries in: a) POM and b) OIM [48,138-140].

TEM clarified the problem.

Although SEM-EBSI appeared about 1980 much after TEM, it is discussed here because of its similarity to POM for Al; the related technique of OIM based on SEM-EBS Scanning Electron Microscopy - Back Scattered Image, diffraction is considered after TEM. In a study of hot compressed Al, (ε = 0.7, 20-500°C, 0.1-200s^{-1}), the SEM images were fairly similar in appearance to the POM results and correlated well with the dimensions measured by TEM [65]. In a broad project, polished specimens of Al and Al-11Zn were examined first by SEM-EBSI and after anodizing by POM; regions identified by microhardness indentations coincided in detail (not the case for Al-5Mg below) [54,66-69]. A study of Al-Mg-Si, showed the development of substructure up to strains of 30; (discussed under ultraductility) [70]. In Cu that had been torsionally strained to ε = 30, EOM distinguished DRX grains (severely quenched) from SRX grains (quenched) mainly by smaller size and indistinct markings [71,72]. The SEM-EBSI and EBSD confirmed the presence of substructure in the DRX grains.

SEM-EBSI of hot worked Al-5.2Mg alloy microstructures were similar to POM but with much clearer definition of each subgrain; SRX grains were clearly defined as they had been in POM of Al-1Mg earlier [51]; at 425°C 2s^{-1} SEM size about 7 μm compared to TEM of 3 μm [73]. In a torsion study of Al-5.2Mg at 400°C $10^{-3}s^{-1}$, POM showed the subgrains developed at ε = 0.5 with strongly serrated GB (Part I: 9,10-DRV). The subgrains remained constant in size as the grains thinned [55]. The serrations become increasingly meandering and some appeared to pinch off, which could be mistaken for DRX [52-54,66-69]. As the grains became ever thinner, $\varepsilon \approx 10$, the billowy serrations appeared like a layer of new grains along the GB [67,69] (called rotation DRX [74]). A TEM study of all the specimens showed that the subgrains were equiaxed and constant in size and misorientation to ε = 16 at fracture [55]. The POM subgrain size was not determined so it was not realized that they were about 4x bigger than the TEM size; this was only confirmed much later [55,67-69]. In another set of experiments to $\dot{\varepsilon}$ = 5 at various T and $\dot{\varepsilon}$, POM exposed subgrains that were larger as T rose, or $\dot{\varepsilon}$ and Z fell, in the extreme, being larger than the grain thickness at low T, high $\dot{\varepsilon}$ or Z, similar to Al even as to size [52, 53]. In the broad project on Al (previous page including Al-11Zn, Al-4.5Mg-0.7Mn), POM subgrains were similar in size in Al and Al-5Mg, but the SEM-EBSI subgrains in Al-5Mg were smaller by a factor of about 4 [54, 67-69]; the SEM ones agreed with TEM ones as explained below. TEM confirmed that the pinched off serrations contained 4-5 subgrains across a diameter; this was identical to those in the neighboring large grains [75, 76]. Clearly these were not DRX nuclei [54] confirming its absence at 5% Mg as in 1-4% as reviewed previously [77].

TRANSMISSION ELECTRON MICROSCOPY TEM

The inception of TEM in the late 1950s finally provided the ability to image individual or grouped dislocations, presenting many surprises of dislocation interactions over an ε range up to ~4. TEM was intensely applied in the 1960's to cold working both to dislocation interactions and to the formation of substructures in an effort to explain strain hardening [28-31,63,78]. As strain increased, tangles formed and transformed into cells that decreased in size with rising strain and

finally saturated in size (~0.5 μm) with an aspect ratio slightly above unity [79] (evidently the cell walls (CW) repeatedly rearrange, as first postulated in hot working [50]). In general, hot work researchers learned much from microstructural development both in cold working and in subsequent annealing. In the 1990's, more careful TEM exposed the formation of geometrically necessary boundaries (GNB, previously called block walls (BW), dense dislocation walls and microbands) (Part I: 11-DRV) that have a spacing of about 5 μm (about 10 cells across) [64,80-83]; many become permanent so their Ψ rises rapidly, being a major cause of strain hardening. Deformation bands with a spacing of 50 μm and larger are seldom noted or distinguished from GB in the limited TEM field of view (Fig. 2, compare to Fig. 1). In hot working Al to be discussed next, the SGB have a spacing of about 5 μm, saturate in Ψ and are transitory, rearranging as ε rises with more facility than cell walls.

TEM provides a god-sent clarification between deformed and non-deformed grains and of hot-worked substructure [11, 14, 15, 22, 48-51, 55, 66-69, 70-72, 84]. In metals, like Al and α-Fe [37,38], the subgrain development up to and through steady state (T, $\dot{\varepsilon}$, σ_S, constant) was clarified with respect to the constancy of the spacings of SGB w (= 0.788 d_S, subgrain diameter) and of the dislocations in them S (= b_v/Ψ) and in the subgrains $\rho_i^{-0.5}$ [66-69,85-87]. The characteristic dependence on T, $\dot{\varepsilon}$ and Z were confirmed with determination of effects of alloying, e.g., in 7075 [22, 33, 61, 69, 73, 88, 89]. Blum and colleagues employed plots of T compensated strain rate and of the above spacings against σ_S/G (G shear modulus); they have shown that this applies to Al alloys [67-69,85-87] and to ferritic and austenitic steels [88]. By this means, they confirmed the unity of creep and hot working mechanisms and the validity of the composite model. In the composite creep model, the stress fields related to spacing of walls and of dislocations in both walls and subgrain interiors are interrelated and together define the flow stress [66-69, 85-87]. An internal forward stress in walls assists dislocations passing through or bowing-out and an internal back stress in the subgrains slows down the migration of mobile dislocations. The progress of SRV under diminishing stress from the softening substructure was charted, including dislocation migration, disintegration of SGB and coalescence of neighboring subgrains into larger ones with higher Ψ [28,29,90]. The constancy of subgrain size, equiaxed shape and misorientation was confirmed in a multitude of tests up to $\varepsilon \approx 4$ [14, 15, 22, 48-50, 66-68] and in special torsion tests up to $\varepsilon = 16$ [55, 91], $\varepsilon = 25$ [92, 93], $\varepsilon = 40$ [94], $\varepsilon = 60$ [95,96] and $\varepsilon \approx 100$ [17, 97, 98] (alternative explanations [94, 96, 99] discussed under serrations and SGB in ultra ductility). These studies, over a span of 30 years, affirmed the rearrangement of SGB through disintegration, (unknitting), reknitting and migration (Figure 2). In addition to exposing simple SGB with tilt or twist orientations, TEM has shown dislocations moving across thin foils, making deviations at SGB and undergoing cross slip in the subgrains in response to SGB stress fields [22, 49, 50]. The subgrain misorientations Ψ were confirmed as low by many neighbor-neighbor selected area diffractions (SAD) and also by rows of up to a dozen subgrains [22, 49, 50]. SAD provided Ψ across individual cellular facets for adding to micrographs; subgrains of similar orientation could be shown by dark-field illumination that was applied to Al-matrix composite exposing wide spatial scatter [100, 101] (OIM can provide even clearer information). Since GB were generally serrated (as were TB), the elongated grains (or deformation bands) could be defined only by (SAD) or by different contrasts through tilting. The presence of TB in the microstructure were determined at strains of 20, 40 and 60 by STEM Kikuchi patterns [95,99].

The persistent equiaxed shape of the subgrains is maintained through continued rearrangement of the SGB by disintegration and reformation, migration and merging [49, 50, 86-88, 95, 96] (Figure 2). High voltage TEM of in-situ straining on a heated stage exhibited the operation of all these mechanisms [102, 103]. This behavior, named repolygonization, clearly pointed out that SGB were very transitory [50, 96, 104, 105]. Change of $\dot{\varepsilon}$ ($\Delta\dot{\varepsilon}$) tests clarified that the substructure rearranged into that characteristic of the new T, $\dot{\varepsilon}$ or Z conditions. The strains to steady state either initially ε_S (0 to σ_S) or in the transient ($\Delta\dot{\varepsilon}_S'$ for $\Delta\sigma'$ due to $\Delta\dot{\varepsilon}'$) were proportional to change in σ [106-109]. It was proposed that in steady state repolygonization is complete each $\Delta\varepsilon = \varepsilon_S$. In hind sight, the TEM microscopy tended to avoid GB in order to report the pure dislocation interactions that had happened inside the grains; there was similar neglect of transition boundaries (TB) between deformation bands (identifiable like grains by contrast in tilting and selected area diffraction, SAD) that being permanent have become serrated and lengthened like GB [95,96,104,105]. The serrations of the GB in response to SGB attraction evidently rearrange in association with repolygonization; this proceeds in association with lengthening of the GB[110].

The subgrain sizes, similar in Al for POM and SEM-EBSI (as mentioned earlier), were slightly larger than those in TEM, because SGB with high values of S having very low Ψ were insufficient to cause noticeable responses in oxide growth or diffraction intensity [54,55,66-69].

Examination of Al-5Mg through low strains showed initial development of planar dislocation arrays that gradually developed cross-links and finally subgrains at strains ε_{SD} well beyond mechanical steady state ε_{SM} [111,112]. Apparently, the walls developed at strains up to ε_{SM} had retained stronger boundaries that controlled the growth of the anodized patches over crystal regions containing 5 subgrains across the diameter (SEM-EBSI agreed fairly well with TEM) [54, 55, 66-69, 111, 112]. While hot working of Al-5Mg to industrial strains always resulted in subgrains [20, 51-55, 66-69, 73, 74, 77], creep tests halted just after ε_{SM} had not [61, 113-115], but more extensive creep compression tests did so [67, 69, 113]. Mg does not lower the SFE but causes solute drag due to Cottrell atmospheres [69]. In the composite model, dislocations in Al-Mg move very slowly across the subgrains, whereas they fly across in Al even though there is considerable back stress from SGB [66,69].

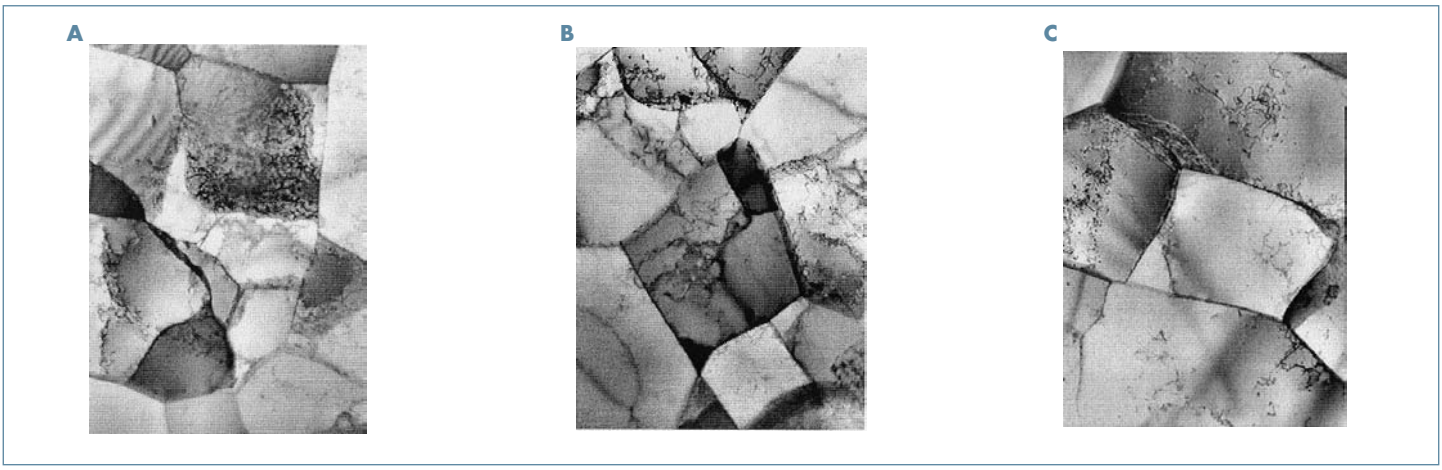

Fig. 2: TEM micrographs of Al deformed at 400°C $0.1s^{-1}$ from regions (normal to radius) near the surface exhibiting similar subgrain structures: a) $\varepsilon = 0.5$; b) $\varepsilon = 1$ and c) $\varepsilon = 0$ (reversed from 0.5) with somewhat reduced internal dislocation density, all at steady state stress 28MPa [48,138-140].

DYNAMIC RECRYSTALLIZATION (EOM, TEM, SEM-EBSI)

TEM also played a role in clearly defining classic discontinuous DRX as occurs in Cu. The detailed progress of classical discontinuous dDRX were described in Part I in stages 1,2,3,4- DRX. In 90% reduction rolling of Cu that finished at 600°C ($0.65T_M$) with a 1-sec quench, the large original grains were thickly decorated along GB with new grains; TEM clearly showed the absence of substructure in these SRX grains [14]. In contrast, the initial grains exhibited fine subgrains with much less DRV than in similarly treated Al that did not exhibit any SRX [14]. The critical strain ε_C is higher for DRX than for SRX because the stress-driven dislocations hamper the developing nuclei that would form during SRV in annealing (Part I: 2-DRX) [116-118]. Torsion testing to 30 at higher T (lower $\dot{\varepsilon}$, Z) and quenching produced fine grains that TEM confirmed as SRX; however, quenching under load just before stopping the motor (an excellent brake) produced very fine grains with a substructure, including also a number of random nuclei starting to grow [71, 72]. The relative sizes of DRX and SRX grains were consistent with mechanical measures of DRX and SRX in low C austenite [119]. TEM of stainless steels deformed in torsion before the peak and in steady state showed that flow stress was related to subgrain size in the same manner (Part I: g-DRX) [120, 121]. From tests on 301,304,316 and 317, the relation of d_S from TEM on Z (or σ_S) [122,123] was similar to the relationship for Al Alloys [121]. The dependence of equilibrium grain size D_S on σ_S [124,125] shows how dislocations reinserted into the new grains seriously curtail GB mobility (Part I: 4-DRV) [116-118,126]; recent experiments confirm that a few lattice dislocations ending on a GB raises its migration activation energy to that for dislocation climb [105,126,127]. In Al given a TMP at $10^{-2}s^{-1}$, nucleation in that substructure does not occur on reducing $\dot{\varepsilon}$ to 10^{-3} or 10^{-4} s^{-1} (development of enlarged d_S, Part I: 8-DRV) but with larger $\dot{\varepsilon}$ reduction, nucleation occurs with longer times and larger grains, indicating the influence of concurrent straining in making nucleation more difficult. [106].

SERRATION AND SGB AT ULTRA-HIGH STRAINS

The microstructural effects to be described were primarily noted in Al polycrystals with normal grains (100 - 200 μm) at high strains (20 - 130) easily attained in torsion at (400 - 550°C) (Part I: 6-SERV) [91-95]; the critical geometric condition is that the elongated grains have thinned down to 2-3 d_S [52, 53, 66-68, 95]. Because of the serrations with half amplitude of ~d_S some neighboring GB come into contact pinching off the grains thus shortening them. The formation of refined grains containing a substructure as a result of grain and cell geometry was called geometric gDRX [95]; in light of the misunderstandings that have arisen, a better name would be grain-defining gDRV [104,105,127]. Because of the serrations, POM exhibits a field of subgrains (or crystallites) that completely masks the grains structure [52-55, 70, 95, 127-129]. TEM exposes the preponderance of SGB with regular dislocation arrays and maintenance of the steady state subgrain size (also confirmed by SEM-EBSI) [54, 66-69, 95]. The mechanical behavior and substructure dimensional parameters were the same at $\varepsilon = 60$ in specimens of 100 μm and 2000 μm; in the latter the grains were still 7 - 10 subgrains thick [95]. In a single crystal subjected to torsion, the substructure Ψ distribution remained stable as ε rose in steady state; however, several TB developed high Ψ, without nucleation [92, 130] in contrast to Cu and Ni which underwent DRX in single crystal torsion (Part I: 7-DRX) [131,132]. An alternative analysis for single phase Al, including all SGB and TB but subtracting lengthened original GB, hypothesizes that the increase in fraction of HAB is evidence of continuous cDRX, in which Ψ of SGB rises with ε so that they became HAB that migrate to combine with each other [70, 94, 128, 129]. This theory does not explain why d_S and σ_S remain constant [70, 96, 127].

XRD of the surface shells (flattened after boring out) from both grain sizes gave the same texture that was analyzed as a deformation one [95, 99, 133] and not a DRX texture, as observed in Cu in steady state after the peak [134,135]. Scanning TEM measures of the micro textures for both grain sizes were the same as the XRD. The scans indicated that, in each grain that had elongated, there were several TB that had rotated into layer bands like the GB

92,95]. In consistence with the geometric changes and elongation of GB and TB, many equiaxed subgrains are in contact with them (as serrations) so that 1/4 to 1/2 of their facets are high angle (without change in σ_S or d_S) [66, 67, 95, 96, 127]. There is also evidence that during high T straining, the slow GB migration associated with serrations also produces a net migration into grains with smaller subgrains (higher Taylor factor), so that they disappear; this accounts for texture evolution (Part I: 5-SERV) [99, 127, 133]. GB are also lost due to migration of triple junctions of the pancaked grains as a result of pinching off in the arms of an acute Y, thus the gDRV mechanism thickens the neighboring grains [85-87]. Similar gDRV (gDRX) phenomenon has been observed in ferritic steels; but one study with carbide decorated initial GB showed a network of MAB, possibly being TB [92,136].

Experiments with varying Z on Al, Al-Mg-Si and Al-5Mg at rising T, or diminishing $\dot{\varepsilon}$, Z, resulted in development of gDRV (or gDRX) at much lower strains as predicted from the theory [52, 53, 67-69, 85, 137]. However, at the highest T and lowest Z, the subgrains with diameter following the normal dependence on Z and flow stress are several times the expected grain thickness (as seen at lower T, higher $\dot{\varepsilon}$, Z) (Part I: 6-SERV); moreover, they appear to remain completely equiaxed [52, 53, 67-69, 127]. Another set of experiments to $\varepsilon > 20$ also confirmed that the grain thickness stabilized near d_S thus dependent on Z developing an equiaxed appearance [92,93]. Finally, in friction stir welding of Al alloys, metal from in front of the advancing pin is sheared to one side in a crescent shaped zone with ε, $\dot{\varepsilon}$ and T declining with distance from the pin, due to constraints from the plates being welded. This crescent material is deposited behind the pin at high T, with $\dot{\varepsilon}$ declining to zero so that the SGB rapidly rearrange to a larger size causing the thinned grains to enlarge with no evidence of nucleation and growth (Part I: 7-SERV) [101]. In Al during steady state torsion at 400°C, 0.1s^{-1}, upon reversal of strain (0.2-0.5-0.2-0), the grains returned to being equiaxed and the SGB and TB remained unchanged with S and ds constant [138].

ORIENTATION IMAGING MICROSCOPY OIM

The OIM provides micrographs calculated from the variations in Kikuchi patterns (SEM-EBS Diffraction) from regions near 0.5 μm square. In torsion experiments, they were observed on polished discs (normal to radius near surface) that were later jetted to perforation for TEM observation; POM examination was later performed on neighboring regions [48, 138, 139]. The substructures were displayed with boundaries selected as: LAB 0.5-5°, MAB 5-15° and HAB 15-180° [105,141]. The HAB (possibly GB) and MAB (possibly TB for ε = 0.2-2) form continuous boundaries, whereas the pattern of LAB (mainly SGB) is incomplete, although their fraction ranges from 0.9 to 0.5, as the strain in Al increases from 0.2 to 6 in the ranges 300 - 500°C 0.1 - 1s^{-1} [48, 139, 140] (Figures 1, 2). The cellular or subgrain sizes (regions classed as grains by the software) range over 3 - 8 μm that are somewhat larger than the TEM subgrains, having similar size ratios as for TEM and SEM-EBSI and thus indicating omission of many low Ψ SGB. The regions that are presented in colors according to their pole position in the basic stereographic triangle, provide some groups of regions defined by HAB or MAB that appear like elongated original grains [48,141]. When colored according to inverse pole figures {with axis either: 1) normal to micrograph [100], 2) at 45° laterally [110] or 3) at 72° towards a corner [111]} regional groups rotated about one such axis are exhibited. Critical analysis of these defines and shows how the original grains are divided into deformation bands, creating the MAB (generally TB) as they rotated [92]. From comparisons of micrographs, many deformation band geometries appear almost identical in POM and OIM [48,92]. In comparison in a TEM specimen at ε = 4, an elongated region exhibited over a dozen equiaxed subgrains with SGB having Ψ = 0.5–5° (av.2.2°) but GB or TB above 15° with the neighboring elongated regions [92,139].

In addition to the above OIM features, the ability to run scans across a region to expose details of the boundaries is perhaps the most enlightening. The scan may provide point-to-point Ψ values so that LAB are like background noise, while MAB exhibit 5-10° and HAB 30-40°. The origin to point cumulative plots exhibit Ψ gradients across some regions, sharp rises and matching drops (MAB) on opposite sides of deformation bands [92] and large random changes at HAB [48]. The scans reinforce the color information so that one can piece together the evolution of grain deformation. In general, the similarities between POM and OIM micrographs are better than between TEM and OIM [48,138-141] (Figure 1).

From the OIM statistics giving dependence on ε up to 6 at 400°C 0.1s^{-1}, the changes in fractions of LAB, MAB and HAB support the theory that Ψ of LAB saturate at about 4° [48,138-140]. From ε = 0.2 to 6, the LAB fraction decrease from 0.8 to 0.5 causing the matching HAB increment, while the MAB remain almost constant near 0.2. This has been explained in Part I: 4-SERV [96,104,105,127,140]. In reverse straining (ε = 0.2-0.5-0.2-0), as the grains return to being equiaxed, the HAB fraction decreases, raising the LAB fraction with little change for MAB; the TB and SGB remain in existence as ε returns to 0. Both forward (as high as ε = 6) and reverse strain take place at constant σ_S and d_S in TEM (Figure 2). The simple OIM micrographs of boundaries distinguished in groups (LAB, MAB, HAB) provide ambiguous evidence open to opposing interpretation [70]. The omission of many very low Ψ LAB causes differences between OIM and TEM; nevertheless, analysis of the changes in statistics for LAB, MAB and HAB with rising strain confirm that LAB are not marching upwards in Ψ but are being replaced by TB or GB as the number of contiguous subgrains rises with elongation. These analyses are clarified in recent reviews [104, 105, 127] and in others with broader analyses [85-87, 96, 127, 142].

SUMMARY

By breaking up the total phenomena of DRV behavior as it proceeds across extreme strains notably in Al and α Fe alloys, it has been possible to see how the different aspects progress with strain as their distinct behaviors are driven by superimposed causes namely plastic stability (deformation bands with transition boundaries) and surface energy (serrations and pinching off). It is notable that despite significant substructural differences between high DRV hot working and cold working, the textures remain closely the same. These varied layers of mechanisms have been clarified through half a century by piecing together the results of etched and polarized light microscopy, of TEM with SAD, SEM-EBS images or diffraction and of OIM.

There were apparent disagreements between the experimental techniques but

with careful analysis they can be brought into mutual clarification and confirmation of the DRV mechanism.

REFERENCES

[1] R.W.K. Honeycombe, Plastic Deformation of Metals, Edward Arnold, London, (1968).

[2] C.S. Barrett, Structure of Metals, 2nd Edition, McGraw-Hull, New York, (1954).

[3] R.F. Mehl, ASM Handbook 1948 Edition, American Society for Metals, Metals Park, OH. (1948), pp. 259-263.

[4] E. Schmid and W.Boas, Plasticity of Crystals, Chapman and Hull, London (1968).

[5] E. C. W. Perryman, Creep and Recovery, ASM, Metals Park, OH. (1957), pp. 111-145.

[6] A. S. Keh, Direct Observations of Imperfections in Crystals, J.B. Newkirk and J.H. Wernick, Interscience Pub., New York (1962), pp. 213-234.

[7] H.J. McQueen, Advances in Metallurgy of Aluminum Alloys, (J.T. Staley Symp.), M. Tiryakioglu, ed., ASM Intl., Materials Park, OH. (2001), pp. 351-360.

[8] H.J. McQueen, (ICAA10 2006, Vancouver), Mat. Res. Forum, 519-523, (2006), 1493-1498.

[9] H.J. McQueen, (ICSMA 13, Budapest), T. Ungar, et al., eds., Mat. Sci. Eng., A387-389 (2004), 203-208.

[10] J.J. Jonas, C.M. Sellars and W.J. McG. Tegart, Metall. Rev., 14 (1969), 1.

[11] J. McQueen and J.J. Jonas, Treatise on Materials Science and Technology, Vol. 6, Plastic deformation of Materials, Academic Press, New York (1975), pp. 393-493.

[12] D. McLean and A. E. L.Tate, Revue Metall., 48 (1951), 765-775.

[13] J. Schey, Acta Techn., Acad. Sc., Hung., 16 (1957), 131-152.

[14] H.J. McQueen, Trans. Japan Inst. Met., 9 Suppl. (1968), 170-177.

[15] J.P. Immarigeon and H. J. McQueen, Can. Metal. Quart., 8 (1969), 25-34.

[16] T. Sheppard, M.A. Zaidi, P.A. Hollinshead, N. Ragarathan, Microstructural Control in Al Alloys, E.H. Chia and H.J. McQueen, Metallurgical Society, Warrendale, PA. (1986), pp. 19-43.

[17] D. Hardwick and W.J. McG. Tegart, Mem. Scient. Revue Metall., 58 (1961), 869-880; J. Inst. Met., 90 (1961-62), 17-21.

[18] H.J. McQueen, E.Evangelista, N.Jin, M.E.Kassner, Metal.Trans. 26A (1995), 1757-1766.

[19] H.P. Stuwe, Z. Metallkde., 56 (1965), 633-642; Acta. Met., 13 (1965), 1337-1342.

[20] J.R. Cotner and W.J. McG. Tegart, J. Inst. Metals, 97 (1969), 73-79.

[21] C. Rossard, Metaux, Corrosion Industries, 35 (1960), 102-115,140-153,190-205.

[22] H.J. McQueen, J.E. Hockett, Met. Trans., 1 (1970), 2997-3004.

[23] W. A. Wood, G. R. Wilms, J. Inst. Metals., 75 (1948-49), 619, 693.

[24] D. McLean, J. Inst. Met. 81, (1952-53), 287-92.

[25] F. Garofalo, Fundamentals of Creep and Creep Rupture in Metals, Macmillan, NY, 1965.

[26] J. W. Kelly, R. C. Gifkins, J. Inst. Met., 82 (1953-54), 475-80.

[27] H. Conrad, Mechanical Behavior of Materials at High Temp., J.E. Dorn, ed., McGraw-Hill, New York (1961), pp. 149-217.

[28] S. Weissman, T. Imura and N. Hosokawa, Recovery and Recrystallization of Metals, Gordon and Breach, New York (1963), pp. 241.

[29] Hsun Hu, Recovery and Recrystallization of Metals, Gordon and Breach, New York (1963), pp. 311-362.

[30] J.L. Lytton, K.H. Westmacott and L. C. Potter, Trans. TMS AIME, 233 (1965), 1757-65.

[31] P.A. Beck, B.G. Ricketts and A. Kelly, Trans. TMS - AIME, 215 (1959), 949.

[32] J.E. Dorn, Creep and Recovery, Am. Soc. Metals, Metals Park, OH. (1957), pp. 255-283.

[33] H.J. McQueen, Metal. Mat. Trans., 33A (2002), 345-362.

[34] J.L. Uvira and J.J. Jonas, Trans-AIME, 242 (1968), 1619-1626.

[35] F.W. Hammad and W. D. Nix, Trans. ASM, 59 (1966), 94-104.

[36] H.J. McQueen, Materials Technology-An Inter-American Approach, ASME N.Y. (1968), pp. 379-388.

[37] E. Evangelista, P. Mengucci, J. Bowles & H.J. McQueen, High Temp. Mat. Proc., 12 (1993), 57-66.

[38] H.J. McQueen, E. Evangelista, P. Mengucci, N.D.Ryan and J.Bowles, Application of Stainless Steels '92, H.Nordberg, J.Bjorklund, eds., Jernkontoret, Stockholm (1992) pp. 924-933.

[39] B. Jaoul, Étude de la Plasticité et Application aux Métaux, Dunod, Paris (1965).

[40] A.F. Brown and R.W.K. Honeycombe, Phil. Mag., 74-1 (1951), 1146.

[41] R.E. Reed-Hill, Physical Metallurgy Principles,Van Nostrand, New York, 1973.

[42] R.W. Cahn, J. Inst. Met., 79 (1951), 129.

[43] G.Y. Chin,Inhomogeneity Plastic Deformation, ASM, Metals Park,OH (1973),pp.83-112.

[44] C.S. Barrett, L.H. Levenson, Trans.AIME, 137 (1990), 112-127.

[45] A. Hone and E.C. Pearson, Metal Progress, 53 (1948), 363.

[46] J.K. Solberg and N. Ryum, Variation in Polarized Light Intensity with Grain Orientation in Anodized Al, Report, Norwegian Technical University, Trondheim, Norway (1984).

[47] F.N. Rhines, Inhomogeneity of Plastic Deformation, ASM, Metals Park, OH. (1973), pp. 251-284.

[48] G. Avramovic-Cingara and H.J. McQueen, Aerospace Materials Manufacturing (and Repairs), Emerging Techniques, Met.Soc.CIM Montreal, M.Jahazi, et al eds. (2006),pp.173-186.

[49] W.A. Wong, H.J. McQueen and J.J. Jonas, J. Inst. Met., 95 (1967), 129-37.

[50] H.J. McQueen, W.A. Wong and J.J. Jonas, Can. J. Phys., 45 (1967), 1225-34.

[51] H.J. McQueen and N. Ryum, Scand. J. Met. 14 (1985), 183-194.

[52] H.J. McQueen, E.V. Konopleva, W. Blum, Microstructural Science, 22 (1995), 299-314.

[53] E. V. Konopleva, H. J. McQueen and E. Evangelista, Materials Characterization, 34 (1995), 251-264.

[54] Q. Zhu, H.J. McQueen and W. Blum, High Temp. Mat. Proc., 17 (1998), 289-297.

[55] G.A. Henshall, M.E. Kassner and H.J. McQueen, Metal. Trans., 23A (1992) 881-889.

[56] J.J. Jonas, H.J. McQueen and D.W. Demiancuk, Deformation Under Hot Working Conditions, Iron Steel Inst., London 1968, pp. 97-99.

[57] G. Avramovic-Cingara and H.J. McQueen, Practical Metall., 30, [1] (1993), pp. 25-39.

[58] J.E. Hatch,Aluminum Properties and Physical Metallurgy, ASM, Metals Park,OH, 1988.

[59] D. McLean: J. Inst. Met. 81, 1952-53, 287-92.

[60] J. Weertman: J. Mech. Phys.Solids, 4, (1956), 230-34.

[61] M.E. Kassner and M.T. Perez-Prado, Fundamentals of Creep in Metals and Alloys, Elsevier, 2004.

[62] W.E. Nix and B. Ilschner, Strength of Metals and Alloys (ICSMA 5), P. Haasen, et al., eds., Pergamon Press, Oxford (1979), pp. 1503-1530.

[63] P.B. Hirsch, R.W. Horne and M.J. Whelan, Dislocations and Mechanical Properties of Crystals, John Wiley, New York (1957), pp. 92.

[64] R.D. Doherty, D.A. Hughes, F.J. Humphreys, J.J. Jonas, D. Juul-Jansen, M.E. Kassner, W.E. King, T.R. McNelley, H.J. McQueen and A.D Rollett, Mat. Sci. Eng., 238 (1998), 219-274.

[65] H.J. McQueen and W.B. Hutchinson, Deformation of Polycastals, N. Hansen et al., eds., Riso Natl. Lab., Roskilde, DK. (1981), pp. 335-342.

ACKNOWLEDGEMENTS

The author wishes to make known that Natural Sciences and Engineering Research Council of Canada has supported his research in hot working for 40 years. As a professor emeritus, he is grateful to the Faculty of Engineering and Computer Science at Concordia University, it has provided space and electronic facilities that were indispensable for the preparation of the paper. He was well assisted by secretaries and technicians and notably by a student, Bonaventure Kilingi. He wishes to thank Tom Bieler for allowing him to bring into a comprehensive picture a clear statement of the behavior in hot working and the problems of microscopic techniques that had been presented in the symposium Dislocations 75 at the TMS Annual Meeting, San Francisco, 2009.

[66] H.J. McQueen, W. Blum, Q. Zhu and V. Demuth, Advances in Hot Deformation, T.R. Bieler and J.J. Jonas, eds., TMS-AIME, Warrendale, PA. (1994), pp. 253-250.

[67] W. Blum, Q. Zhu, R. Merkel and H.J. McQueen, Z. Metalkde, 87 (1996), 14-23.

[68] W. Blum, Q. Zhu, R. Merkel and H.J. McQueen, Mat. Sci. Eng., A205 (1996), 23-30.

[69] H.J. McQueen and W. Blum, Aluminium 80, <10>, (2004), 1151-1159, <11>, 1263-1270, <12>, 1347-1355.

[70] S. Gourdet, C. Chovet and H.J. McQueen, Aluminum Transactions 3 (2001), 59-68.

[71] H.J. McQueen and S. Bergerson, Met. Sci. J., 6 (1972), 25-29.

[72] L. Gavard, M. Montheillet and H.J. McQueen, Proc. ICOTOM 12, J.A. Szpunar, ed., NRC Res. Pub., Ottawa (1999), pp. 878-883.

[73] E. Cerri, E. Evangelista and H.J. McQueen, High Temp. Mat. Proc., 18 (1999), 227-240.

[74] F.J. Humphreys and M.R. Drury, Aluminum Technology, T. Sheppard, et al., Inst. Metals, London, (1986), pp.191-196.

[75] I. Samajdar, P. Ratchev, B. Verlinden, P. Van Houtte, P. DeSmet, Mater. Sci. Eng., A247 (1998), 58-66.

[76] H.J. McQueen and E.Evangelista, Czech. J. Phys., 1988, B38, 359-372.

[77] H.J. McQueen, E. Evangelista and M.E. Kassner, Z. Metallkde., 82 (1991), 336-345.

[78] F.R.N. Nabarro, Z S. Basinski and D.B. Holt, Adv. Phys., 13 (1964), 193-323.

[79] F. Schuh and M. Von Heimendahl, Z. Metallkde, 65 (1974), 346.

[80] B. Bay, N. Hansen, D.A. Hughes and D. Kuhlmann-Wilsdorf, Acta.Metal.Mat., 40 (1992), 205-219.

[81] D.A. Hughes and A. Godfrey, Hot Deformation of Al Alloys II, T.R. Bieler, et al., eds. TMS, AIME, Warrendale, PA. (1998), pp. 23-36.

[82] N. Hansen and D. Juul-Jensen, Hot Working of Al Alloys, T.G. Langdon, et al., eds. TMS AIME, Warrendale, PA. (1991), pp. 3-20.

[83] W. Pantleon (IPSMA 10), Mat. Sci. Eng., A462 (2006).

[84] H.J. McQueen, Superplasticity and Superplastic Forming Technology, D.G. Sanders, D.C Dunand, eds., ASM International, Metals Park, OH. (2001), pp. 154-163.

[85] W. Blum and H.J. McQueen, Aluminum Alloys Physical and Mechanical Properties. ICAA5, J.H. Driver, et al., Mat. Sci. Forum, 217-222 (1996), 31-42.

[86] H.J. McQueen and W. Blum, Recrystallization and Related Topics, Rex '96, T.R. McNelley, ed., Monterey Inst. Advanced Studies, CA. (1997), pp. 123-136.

[87] H.J. McQueen and W. Blum, Al Alloys Physical and Mechanical Properties, (ICAA6), T. Sato, ed., Japan Inst. Metals (1998), pp. 99-112.

[88] W. Straub and W. Blum, Hot Workability of Steels and Light Alloys-Composites. H.J. McQueen, E.V. Konopleva N.D. Ryan, eds., Met. Soc. CIM, Montreal (1996), pp. 189-201.

[89] E. Cerri, E. Evangelista, A. Forcellese, H.J.McQueen, Mat.Sci.Eng., A197 (1995), 181-198.

[90] T. Hasogawa, T. Yakou and U.F. Kocks, Acta Metal., 30 (1983) 235-243.

[91] H.J. McQueen, G. Avramovic-Cingara and P. Sakaris and A. Cingara, Proc. 3rd Intnl. SAMPE Metals Conf., (Toronto), (1992), pp. M192-M206.

[92] H.J. Mcqueen (Int Conf Strength Maerials, Dresden 2009, w. Skrotzki etal. eds.), J. Physics, Conference Series, 240 (2010) http//iopscience.iop.org/1742-6596/240/1/9120062010).

[93] T. Petterson and E. Nes, Metal. Trans. 34A (2003), 2727-2736. Add from ref. 92 pages 2737-2744 to ref 93 as additional pages 2727-2736,2737-2744.

[94] Ch. Perdrix, M.Y. Perrin, F. Montheillet, Mem. Et. Sci. Rev. Métal., 78 (1981), 309-320.

[95] J.K. Solberg, H.J. McQueen, N. Ryum and E. Nes, Phil. Mag., 60 (1989), 447-471.

[96] H.J. McQueen, W. Blum, Mat. Sci. Eng., A290 (2000), 95-107.

[97] Y.A. Likhachev, M.M. Myshlyaev, S.S. Olevski, and T.N. Chuchman, Acta Metal., 22 (1974), 829-834.

[98] M.E. Kassner, M.M. Myshlyaev and H.J. McQueen, Mat. Sci. Eng., A108 (1989), 45-61.

[99] H.J. McQueen, Proc. ICOTOM 12, J.A. Szpunar, ed., NRC Res. Pub., Ottawa (1999), pp. 836-841.

[100] M.M. Myshlyaev, E. Konopleva and H.J. McQueen, Mat. Sci. Tech., 1998, 14, 939-948.

[101] X. Xia and H.J. McQueen, Microstructural Science, 22, (1995), 285-296.

[102] V.K. Lindroos, H.M.Miekk-oja, Phil. Mag., 16 (1967), 593-610; 17 (1968), 119-33.

[103] D. Caillard and J.L. Martin, Acta Met., 31 (1983), 813-825.

[104] H.J. McQueen, M. Cabibbo, E. Evangelista, Mat. Sci. Tech., 23 (2007), 803-809.

[105] H.J. McQueen and S. Spigarelli, Mat. Sci. Eng., A462 (2007), 37-44.

[106] Y. Huang and F.J. Humphreys, Acta Mater., 45 (1997), 4491-4503.

[107] I. Fereira and R.G. Stang, Acta Met. 31 (1983), 585.

[108] W. Blum and A. Finkel, Acta Met., 30 (1982), 1705-1715.

[109] W. Blum and H. Schmidt, Res. Mech. 9 (1983), 105.

[110] H.J. McQueen, N.D. Ryan, E.V. Konopleva, X.Xia, Can.Metal.Quart.,34(1995),219-229.

[111] I. Poschmann and H.J. McQueen, Scripta Metal. Mat. 35, (1996), 1123-1128.

[112] H.J. McQueen and I. Poschmann, Strength of Materials, ICSMA 11 (Prague 1997, P. Lukacs, ed.) Mat. Sci. Eng. A234-236, (1997), 830-833.

[113] E. Wekert and W. Blum, Strength of Metals and Alloys (ICSMA 7), H.J. McQueen, et al. eds, Pergamon Press, Oxford (1985), pp. 773-778.

[114] H. Oikawa, K. Sugawara and S. Karashima, Trans. J. Inst Metals 19 (1978), 611.

[115] T.G. Langdon, Strength of Metals and Alloys, R.C. Gifkins, ed., Pergamon Press, Oxford (1982), pp. 1105-1120.

[116] H.J. McQueen, Mat. Sci. Eng., A101 (1987), 149-160.

[117] H.J. McQueen, Recrystallization '92, M.Fuentes, J.Gil Sevillano, eds., Trans Tech. Pub., Switzerland, (Mat.Sci.Forum, 113-115, 1993), (1992), pp. 429-434.

[118] H.J. McQueen and D.L. Bourell, Inter-relationship of Metal. Structure and Formability, A.K.Sachdev, J.D. Embury, eds., Met. Soc. AIME, Warrendale, PA. (1987), pp. 341-368. J. Met., 39 [9] (1987), 28-35.

[119] H.J. McQueen, S. Yue, N.D. Ryan and E. Fry, J. Mat. Proc. Tech. 53 (1995), 293-310.

[120] L.Fritzmeier, M. Luton and H.J. McQueen, Strength of Metals and Alloys (ICSMA 5, Aachen) P. Haasen et al., eds. Pergamon Press, Frankfurt (1979) Vol. 1, pp.95-100.

[121] H.J. McQueen, Thermomechanical Processing of Steel (Jonas Symposium), S. Yue, E. Essadiqi, eds., Met. Soc. CIM, Montreal (2000), pp. 323-333.

[122] N.D. Ryan, H.J. McQueen, J. Mat.Proc.Tech., 21 (1990) 177-199; 30 (1993) 103-123.

[123] E. Evangelista, N.D. Ryan, H.J. McQueen, Metal. Sci. Eng., 5 [2] (1987) 50-58.

[124] C.M. Sellars, Phil. Trans. Roy. Soc., A288 (1978), 147-158.

[125] T. Sakai and J.J. Jonas, Acta Metall., 32 (1984), 189-209.

[126] M. Winning, Recrystallization and Grain Growth, Verlag (2001), G. Gottstein and D.A. Molodov, Springer, pp. 21-38,193-204.

[127] H.J. McQueen and M.E. Kassner, Scripta Mater, 51, (2004), 461-465.

[128] S. Gourdet and F. Montheillet, Mat. Sci. Eng., A283 (2000), 274-288.

[129] S. Gourdet and M. Montheillet, Acta Mater., 51 (2003), 2685-2699.

[130] M.E. Kassner, Metal.Trans, 20A (1989), 2182-2185.

[131] G. Gottstein, Met. Sci., 17 (1983), 497-502.

[132] P. Karduck, G. Gottstein and H. Mecking, Acta Metal., 31 (1983), 1525-1536.

[133] G.R. Canova, U. Kocks and J.J. Jonas, Acta Metal., 32 (1984), 211-226.

[134] E. Aernoudt and H.-P. Stuwe, Z. Metallk., 61 (1970), 128-136.

[135] F. Montheillet, M. Cohen, J.J. Jonas, Acta Metal., 32 (1984), 2077-2089.

[136] R Lombry, C. Rossard and B. Thomas, Rev. Met., 78 (1981), 975-988.

[137] I. Guttierez and M. Fuentes, Recrystallization '90, T. Chandra, ed., TMS-AIME, Warrendale, PA. (1990), pp. 807-812.

[138] G. Avramovic-Cingara and H.J. McQueen, (ICAA10 Vancouver), Mat. Res. Forum, 519-523 (2006), pp. 1659-1664.

[139] G. Avramovic-Cingara, H.J. McQueen and D.D. Perovic, Light Metals/Metaux Legers 2004, D. Gallienne, R. Ghomaschi eds., Met. Soc., CIM, Montreal (2004), pp. 141-152.

[140] H.J. McQueen B. Anandapadmanaban and G. Avramovic-Cingara, Light Metals in Transport Applications, Met. Soc. CIMM, Montreal, (2007), pp. 297-308.

[141] Kh.A.A. Hassan, A.F. Norman and P.B. Prangnell, 3rd Int. Symp. On Friction Stir Welding, Sept. (2001) Kobe, Japan (on CD).

[142] H.J. McQueen, Aluminum Alloys: Physical Mechanical Properties, ICAA9, J.F. Nie, et al., eds., Monash Univ. Melbourne, Australia, (2004), pp. 351-356.